DNA-cytometry of progressive and regressive cervical intraepithelial neoplasia

Antonius G.J.M. Hanselaar[a], Neal Poulin[b], Martin M.M. Pahlplatz[a], David Garner[b],
Calum MacAulay[b], Jasenka Matisic[b], Jean LeRiche[b] and Branko Palcic[b]

[a]*Department of Pathology, University Hospital Nijmegen, P.O. Box 9101, 6500 HB Nijmegen,
The Netherlands*
[b]*Cancer Imaging Department, Medical Physics Division, British Columbia Cancer Agency,
Vancouver, BC, Canada V5Z 1L3*

Abstract. A retrospective analysis was performed on archival cervical smears from a group of 56 women with cervical intraepithelial neoplasia (CIN), who had received follow-up by cytology only. Automated image cytometry of Feulgen-stained DNA was used to determine the differences between progressive and regressive lesions. The first group of 30 smears was from women who had developed cancer after initial smears with dysplastic changes (progressive group). The second group of 26 smears with dysplastic changes had shown regression to normal (regressive group). The goal of the study was to determine if differences in cytometric features existed between the progressive and regressive groups. CIN categories I, II and III were represented in both groups, and measurements were pooled across diagnostic categories. Images of up to 700 intermediate cells were obtained from each slide, and cells were scanned exhaustively for the detection of diagnostic cells. Discriminant function analysis was performed for both intermediate and diagnostic cells. The most significant differences between the groups were found for diagnostic cells, with a cell classification accuracy of 82%. Intermediate cells could be classified with 60% accuracy. Cytometric features which afforded the best discrimination were characteristic of the chromatin organization in diagnostic cells (nuclear texture). Slide classification was performed by thresholding the number of cells which exhibited progression associated changes (PAC) in chromatin configuration, with an accuracy of 93 and 73% for diagnostic and intermediate cells, respectively. These results indicate that regardless of the extent of nuclear atypia as reflected in the CIN category, features of chromatin organization can potentially be used to predict the malignant or progressive potential of CIN lesions.

Keywords: Uterine cervix, dysplasia, image analysis, automation, DNA

1. Introduction

Since the introduction of cytological diagnosis of cervical (pre-)malignant lesions, the surface of the uterine cervix has become one of the most extensively examined areas of the human body. Dysplastic cellular changes can be identified in cytological smears, and thus selected women can be treated in an early phase before further signs or symptoms have occurred. Organized screening has significantly contributed to the reduction, incidence, and mortality from cervical cancer [1,16,24,25,27,28]. This success, however, has come at the cost of treating too many women. Most women who are treated for dysplasia would never have developed cancer, because the lesions would have regressed spontaneously

to normal [16]. The problem of over-treatment continues to worsen. The management of the atypical squamous cells (ASCUS category of the Bethesda classification system, Papanicolaou class 2) has become increasingly aggressive [12,14,31]. This approach is likely to very ineffective and expensive, and to create much anxiety among women.

Data from the screening program in the Netherlands illustrate the discrepancy between the number of positive smears and the incidence of cervical cancer (Table 1). In the Netherlands each year about 400,000 women are being screened after invitation by the screening organizations, out of a population of 3,200,000 women at risk between the age of 30 and 60 years [32]. An estimated 12,500 women will have "positive" follow-ups and are candidate to be treated [13]. The calculated incidence of invasive cervical cancer is, however, much lower, e.g., 120–200 per 400,000 women in this age group [29]. From these data it is obvious that routine cytomorphologic classification of smears does not have the power to recognize only those patients who have a high probability to develop cancer.

In a previous image analysis study we have analyzed diagnostic cells within Feulgen-stained smears of patients who, after initial smears showing dysplasia, had developed cancer. We indicated that image analysis may be helpful to discriminate between progressive and non-progressive intra-epithelial changes of the cervix [11]. Furthermore, image analysis of Malignancy Associated Changes (MAC's) as present in normal appearing intermediate cell has been shown to be of value to identify co-occurent dysplastic changes [23].

In the present study of archival material we performed image cytometric analysis of diagnostic and intermediate cells as present within 56 Feulgen-stained smears. The first group of 30 smears was from women who had developed cancer after initial smears with dysplastic changes. The second group of 26 smears with dysplastic changes had shown regression to normal. Since these women did not receive treatment (until the development of invasive carcinoma in the progressive group), the lesions in this study group are representative of the natural history of CIN. The aim of this study was to determine whether image cytometric analysis could help to discriminate between these two groups of progressive and regressive lesions, and to test whether DNA-cytometric features could help to correctly classify such lesions as being progressive or regressive.

Table 1
Cervical screening in the Netherlands

Cases per year	Description of population
Number of screened women	
3,200,000	Women at risk between 30 and 60 years of age
380,000–450,000	Number of women screened per year (60–70% attendance; 5-year interval)
±50,000	"Non-negative" smears by initial cytology (12% of smears are initially called "non-negative" and followed up)
±12,500	Cases are "positive", either in initial smear, or on follow-up (assumes 25% of "non-negative" smears have "positive" follow-up; women are referred to gynecologists)
Calculated number of women with invasive cancer of the cervix	
960–1,600	Calculated number of cases of invasive cancer per 3,200,000 (assumes 30–50 cases of cancer per 100,000 women between 30 and 60 years in unscreened population)
120–200	Calculated incidence of cases of cancer per 400,000 women

2. Material and methods

2.1. Patient group

From the archives of the department of cytopathology of the British Columbia Cancer Agency (BCCA), two groups of smears were selected (Table 2). The first group contained 30 smears of successive patients who, after previous cervical smears consistent with CIN I, II or III, had developed an invasive squamous cell carcinoma of the cervix that was histologically diagnosed in 1988. The mean time interval between the cytologic diagnosis of CIN and histologic diagnosis of cancer was 24 months (range: 1–89 months). The CIN lesions of these patients (13 cases of CIN I, 9 cases of CIN II, 8 cases of CIN III) are labeled with the prefix "pro" for their progressive course. The mean age of the patients at diagnosis of a pro-CIN lesion was 42.0 years (range: 24–86 years).

The second group contained 26 smears of women, who had been followed by cytology only. The mean time interval between the cytologic diagnosis of CIN and two successive normal smears was 87 months (range: 43–128 months). The CIN lesions of these patients (two cases of CIN I, 14 cases of CIN II, 11 cases of CIN III) are labeled with the prefix "reg" for their regressive course. The mean age of the patients with a reg-CIN lesion was 33 years (range: 19–66 years).

2.2. Cytologic material

Cytologic smears had been routinely prepared by scraping the surface of the cervical mucosa with a wooden spatula. The material was then put on slides, air dried, and stained according to the Papanicolaou technique for routine diagnostic purposes. The initial cytologic diagnosis was accepted as the reference diagnosis. All slides that were accepted for this study were reviewed by a cytopathologist. For cytometric analysis the coverslips of the slides were removed using xylol and the specimens were then rehydrated according to the following sequence, ethanol 96% (twice), ethanol 70%, ethanol 40% and distilled water. Thereafter specimens were de-stained in a mixture of methanol, 37% formaldehyde and acetic acid (85 : 10 : 5 by volume) for one hour, rehydrated, treated with acid hydrolysis (5 N HCl) at 22°C for 60 min and re-stained using the (Thionin-SO_2) Feulgen procedure. No cytoplasmic counterstain was used.

2.3. Image acquisition

Image acquisition was performed using the Oncometrics Cyto-Savant™ automated quantitative image cytometer (Oncometrics Imaging Corp., Vancouver, BC, Canada). This includes a 12 bit Micro

Table 2
The total number of smears and of intermediate and diagnostic cells selected for each of the diagnostic subgroups

Diagnostic subgroup	N smears	Intermediate cells	Diagnostic cells
pro-CIN I	13	4168	590
pro-CIN II	9	2751	493
pro-CIN III	8	983	788
Subtotal	30	7902	1,871
reg-CIN I	2	174	16
reg-CIN II	13	2336	565
reg-CIN III	11	1318	1,010
Subtotal	26	3828	1,591
Total	56	11,730	3,462

Imager 1400 digital camera (picture elements 6.8 μm $\times$ 6.8 μm), an automated pneumatic slide loader, and a motorized xyz-stage. Thionin-Feulgen-stained nuclei were measured with monochromatic light at a wavelength of 600 nm (band width 10 nm), using a 20 $\times$ 0.75 N.A. PlanApo objective lens. The effective pixel size was 0.34 μm $\times$ 0.34 μm. Nuclei were automatically located in the digital images using a grey level thresholding procedure to locate all objects, followed by a refined individual cell focusing algorithm. Finally, the segmentation of the object was standardized using an edge relocation algorithm to precisely place the edge of the object at the region of highest local grey level gradient [17].

2.4. Cell selection

Using a subset of the 126 nuclear features measured with the cytometer, a cell classification function was applied to the data as the scan proceeded, and 4 classes of objects were distinguished: (1) intermediate cells, (2) diagnostic cells, (3) lymphocytes, and (4) debris. The slides were scanned exhaustively to detect all diagnostic cells and until a specified number of lymphocytes and intermediate cells were obtained. Images of all epithelial cells were re-classified by a cytotechnologist in order to refine the machine classification.

2.5. Image analysis

Nuclear features were extracted from the digitized nuclear images of each selected cell. The 126 features were calculated using the procedure incorporated within the Oncometrics Cyto-Savant™ image cytometer [9]. These features can be classified into six different feature groups: (1) morphometric – describing the size and shape of the nucleus; (2) photometric – describing the distribution of optical density within the stained nucleus, including the integrated optical density (IOD, proportional to the DNA content); (3) discrete texture – relying on the division of nucleus into regions of high, medium, and low chromatin condensation states, and describing the spatial distribution and photometric properties of these regions; (4) Markovian texture – features which characterize the distribution of grey level intensity values between adjacent pixels in the image; (5) run-length texture – features which describe the length of contiguous regions with constant grey level intensity, as well as the photometric properties of these regions; and (6) fractal texture, which measure the surface area of the 3D plot of optical intensity vs. x-y position of the pixels in the nuclear image.

2.6. Statistical analysis

For the statistical analyses of the intermediate cells all 56 smears (30 smears with pro-CIN and 26 smears with reg-CIN) were accepted. For the analysis of the diagnostic cells, 46 smears were accepted in which 15 or more diagnostic cells had been detected (26 pro-CIN; 20 reg-CIN). Because of the relatively small number of cases within each of the progressive and regressive subgroups, all pro-CIN I, II and III lesions were pooled to form one group (pro-CIN) for the analysis, as were all reg-CIN I, II and III lesions (reg-CIN group). A stepwise linear discriminant analysis was used to select those DNA-cytometric features that could discriminate between individual cells of the pro-CIN and reg-CIN lesions (using multivariate statistics F-to-Enter and F-to-Remove). Two separate discriminant analyses were performed using feature values of (1) diagnostic cells, and (2) intermediate cells. For each group of cells the discriminant analysis was performed with selection of a subset of features from the 126 Oncometrics parameters. The resulting discriminant functions were used to classify each of the cells on the slide as positive or negative for progression associated changes (PAC). The slides were

then classified by setting a threshold on the percentage of PAC-positive cells detected. This threshold was selected to maximize the slide classification accuracy as "progressive" or "regressive". An alternative method for slide classification was also investigated. For each slide, means and variances of the feature measurements were calculated, and these parameters were used as input to stepwise discriminant function analysis for slide classification.

2.7. DNA histograms

The DNA content of nuclei, expressed as DNA index, is defined as the normalized measure of integrated optical density of a nucleus. Normalization was performed using internal controls cells, by dividing the DNA content of the nucleus by the median value of the DNA content of leukocytes, present on each slide. The staining intensity over this series of archival slides varied considerably: the median values of integrated optical densities (MD IOD) of the internal control cells ranged from 58 to 147 (mean: 105, 95% confidence interval: 100–110). The mean value of the coefficient of variation of the controls was 16.7%, which exceeds the recommendations of the ESCAP consensus conference on cytometry of DNA content [5]. This large CV is due to the archival nature of the specimens available for analysis, and indicates that the sensitivity of ploidy determinations is compromised in this series. DNA histograms were displayed using a bin-size of 0.05. Two types of DNA histograms were compiled: (1) DNA histograms of all diagnostic cells per slide of all cases with 15 or more diagnostic cells; and (2) DNA histograms of diagnostic cells combined from different slides within diagnostic (sub)groups: e.g., pro-CIN I, pro-CIN II, etc., and all cells combined from pro-CIN lesions and reg-CIN lesions. The DNA ploidy patterns of each case was visually classified as DNA-diploid, DNA-polyploid, or DNA-aneuploid, according to definitions as described previously [11].

The DNA index (DI) is defined as the DNA content of the cell divided by the mean DNA content of the internal diploid control cells, so that a DI of 1.0 corresponds to a diploid cell. DI values greater than 1.25 are taken to be aneuploid.

The 2.5c and 5c exceeding rates (ER) were defined as the percentages of diagnostic cell nuclei per specimen, with DI values of DI > 1.25 and DI > 2.5, respectively. The mean and CV of the DNA index over the diagnostic cells were also determined. The entropy of the DNA histogram, representing the information content, or disorder of the histogram, was determined according to the formula

$$\text{entropy} = -\sum_i p_i \log p_i,$$

where p_i is the proportion of cells within histogram bin i, and where the sum $\sum_i$ is taken over all bins in the histogram. All DNA histograms were compiled using 100 bins over an interval of DI from 0.0 to 5.0.

3. Results

3.1. Classification of diagnostic cells

The results of the stepwise linear discriminant analysis of the diagnostic cells to discriminate between pro-CIN and reg-CIN lesions are shown in Table 3. A number of morphometric features showed significant differences between cells from pro-CIN and reg-CIN lesions, the most discriminating of which are listed below:

Table 3

Classification matrix for diagnostic cells. Performance of discriminant function derived from diagnostic cells from pro-CIN and reg-CIN lesions

Group	% Correct	Number of cells classified into group	
		Progressive	Regressive
Progressive	89	1665	206
Regressive	73	430	1161
Total	82	2095	1367

– OD max: the largest value of the optical density of the object, normalized against the slide mean of the iod (iod-norm);
– Mean radius: the mean value of the distance from the centroid of the object to the object edge;
– Med DNA amnt: a discrete texture feature representing the total DNA content of regions of medium-condensed chromatin;
– Range extreme: the difference between the largest local maximum and the smallest local minimum of optical intensity within the nucleus, normalized against (iod-norm);
– Center of gravity: represents the distance from the geometrical center of the object to the "center of the mass" of the optical density function, normalized by the mean radius of the object. Large values of this feature indicate asymmetry of the optical density distribution over the nucleus;
– Fractal area 1: this feature is derived through analysis of the 3D plot of the optical intensity vs. the x and y spatial coordinates of the cell image. The fractal area is the surface area of this plot, and represents the complexity of the optical density distribution (e.g., a cell with completely smooth OD distribution will have a smaller fractal area than a cell with alternating patches of light and dark chromatin). Fractal area 1 is the surface area at full image resolution;
– Run length 90: this run length texture feature is a measure of the number of consecutive pixels in the image with constant grey level, giving another estimate of the uniformity of optical density distribution in the nucleus. In this case, the runs of constant grey level are computed in the vertical direction, denoted by the 90 in the feature title.

Using the diagnostic cells of the pro-CIN and reg-CIN lesions a discriminant function was derived based on three selected features (mean radius, med DNA amount, range extreme), with overall classification accuracy between progressive and regressive lesions of 82%. The resulting classification matrix is shown in Table 3. Using a jackknife procedure, the cells of pro-CIN lesions were classified correctly in 89% of cases, the cells of the reg-CIN lesions in 73% of cases. The performance of the discriminant function without the jackknife procedure was virtually equivalent.

Figure 1 shows a plot of the discriminant function derived from diagnostic cells from the pro-CIN and reg-CIN lesions. The selected features exhibit a high heterogeneity in the regressive lesions, showing three distinct peaks, whereas the plot of the progressive lesions is essentially unimodal.

The stability of all discriminant analyses was evaluated by splitting the sample in half and by using the discriminant function derived from one half to classify the other half (and vice versa). The features used in these analyses were forced to be identical to those which comprised the original discriminant function. For the CIN lesions analyzed in this manner, the jackknifed classification accuracies were 80.4 and 79.8% for the two halves of the data, confirming that the features provide a stable discrimination between the progressive and regressive groups.

Classification of slides was performed using two different methods. In the first, discriminant analysis was performed using the mean and variance of feature measurements over individual slides. With this
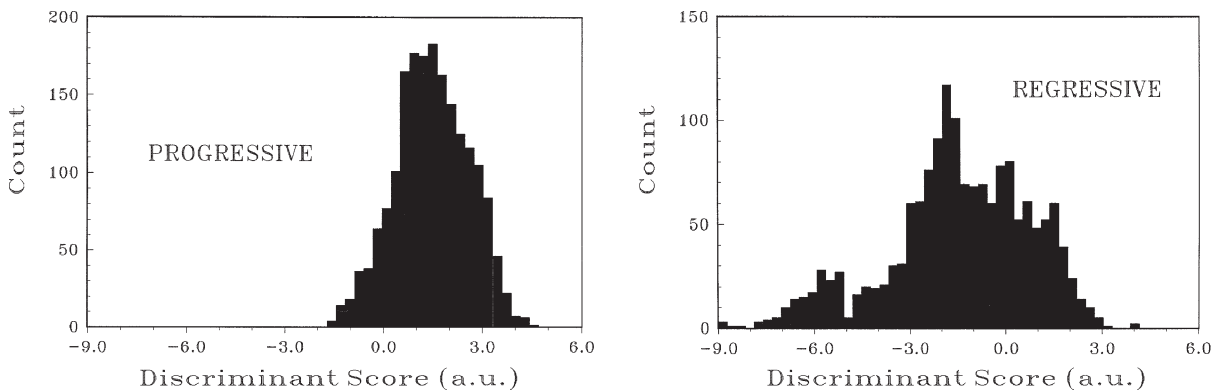
Fig. 1. Discriminant score derived from diagnostic cells from pro-CIN and reg-CIN lesions.

method, the dimensionality of the feature space is restricted by the small number of cases. Allowing two of the most discriminating variables to be entered into the discriminant function, a classification accuracy of 75% is achieved for diagnostic cells. The jackknifed classification accuracy using these two variables is 69%, suggesting that this analysis is not stable due to the small sample size.

Analysis of the feature means and variances may tend to obscure the existence of subpopulations of cells which may be more likely to establish a progressive clone. More insight into the distribution of feature measurements can be gained if we analyse the behavior of the cell discriminant function over the population of cells within individual slides. In this case classification of each slide is performed by thresholding the percent of cells positive for progressive associated changes on each slide (PAC, defined as a cell with discriminant score >0). The classification accuracy, using diagnostic cells from 46 slides, was 93% at a threshold of 80% PAC$^+$ cells. For pro-CIN ($N = 26$) the classification accuracy was 96%. For reg-CIN ($N = 20$) the classification accuracy was 90%.

Figure 2 shows typical examples of diagnostic cells of, respectively, PAC$^+$ nuclei from pro-CIN lesions and PAC$^-$ nuclei from reg-CIN lesions.

3.2. Classification of intermediate cells

The results of the stepwise linear discriminant analysis of the intermediate cells to discriminate between pro-CIN and reg-CIN lesions are shown in Table 4. The following set of features were shown to exhibit the most significant differences:

- Mean radius;
- DNA index;
- Low DNA area: a discrete texture feature representing the ratio of the area of the low optical density regions of the object to the total object area. Analogous definitions exist for medium and high density DNA areas;
- Medium average distance: this feature represents the asymmetry of the distribution of medium density chromatic, and measures the average distance of pixels representing medium density chromatin from the geometric centre of the object;
- High density objects: the number of distinct particles of high density chromatin;
- Contrast: a Markovian feature which emphasizes the contrast between adjacent pixel intensities. This feature is highest for objects with large variations between adjacent pixels;
- Range extreme (see above).

(a)

(b)

Fig. 2. Images of digitized nuclei of Feulgen-stained diagnostic cells of (a) pro-CIN and (b) reg-CIN lesions.

Table 4
Classification matrix for intermediate cells. Performance of discriminant function derived from intermediate cells from pro-CIN and reg-CIN lesions

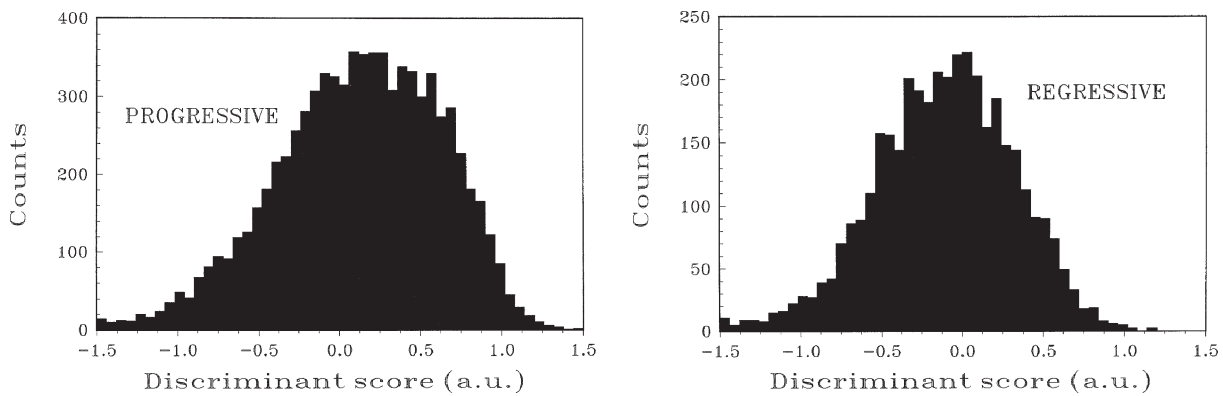| Group	% Correct	Number of cells classified into group	
		Progressive	Regressive
Progressive	60.8	4803	3099
Regressive	58.9	1574	2254
Total	60.1	6509	5221

Fig. 3. Discriminant score derived from intermediate cells from pro-CIN and reg-CIN lesions.

Using the intermediate cells of the pro-CIN and reg-CIN lesions a discriminant function was derived allowing 4 of the most discriminating variables to be entered (medium average distance, high density objects, contrast, and range extreme). The overall cell classification accuracy between progressive and regressive lesions was 60%, considerably lower than that for diagnostic cells. The resulting classification matrix is shown in Table 4. Using a jackknife procedure, the intermediate cells of pro-CIN lesions were classified correctly in 61% of cases, the cells of the reg-CIN lesions in 59% of cases. Stability of discriminant analysis was again confirmed by dividing the sample in half.

Figure 3 shows a plot of the discriminant function derived from intermediate cells from the pro-CIN and reg-CIN lesions. In contrast to the diagnostic cell analysis, the overlap between the two groups is considerable, and both plots show an essentially unimodal distribution. Also in contrast to the analysis of diagnostic cells, the variability in the discriminant score for regressive lesions is comparable to that for the progressive.

Slide classification was again performed by thresholding the percent of PAC$^+$ cells on each slide. The classification accuracy, using intermediate cells, was 73% at a threshold of 40% PAC$^+$ cells. For pro-CIN the classification accuracy was 70%. For reg-CIN the classification accuracy was 76%.

The accuracy was similar when slide classification was performed using feature means and variances as input variables to discriminant function analysis. With feature selection for the set of two most discriminating variables, the accuracy was 70% for both jackknifed and non-jackknifed classifications.

Figure 4 shows typical examples of intermediate cells from pro-CIN and reg-CIN lesions, respectively.
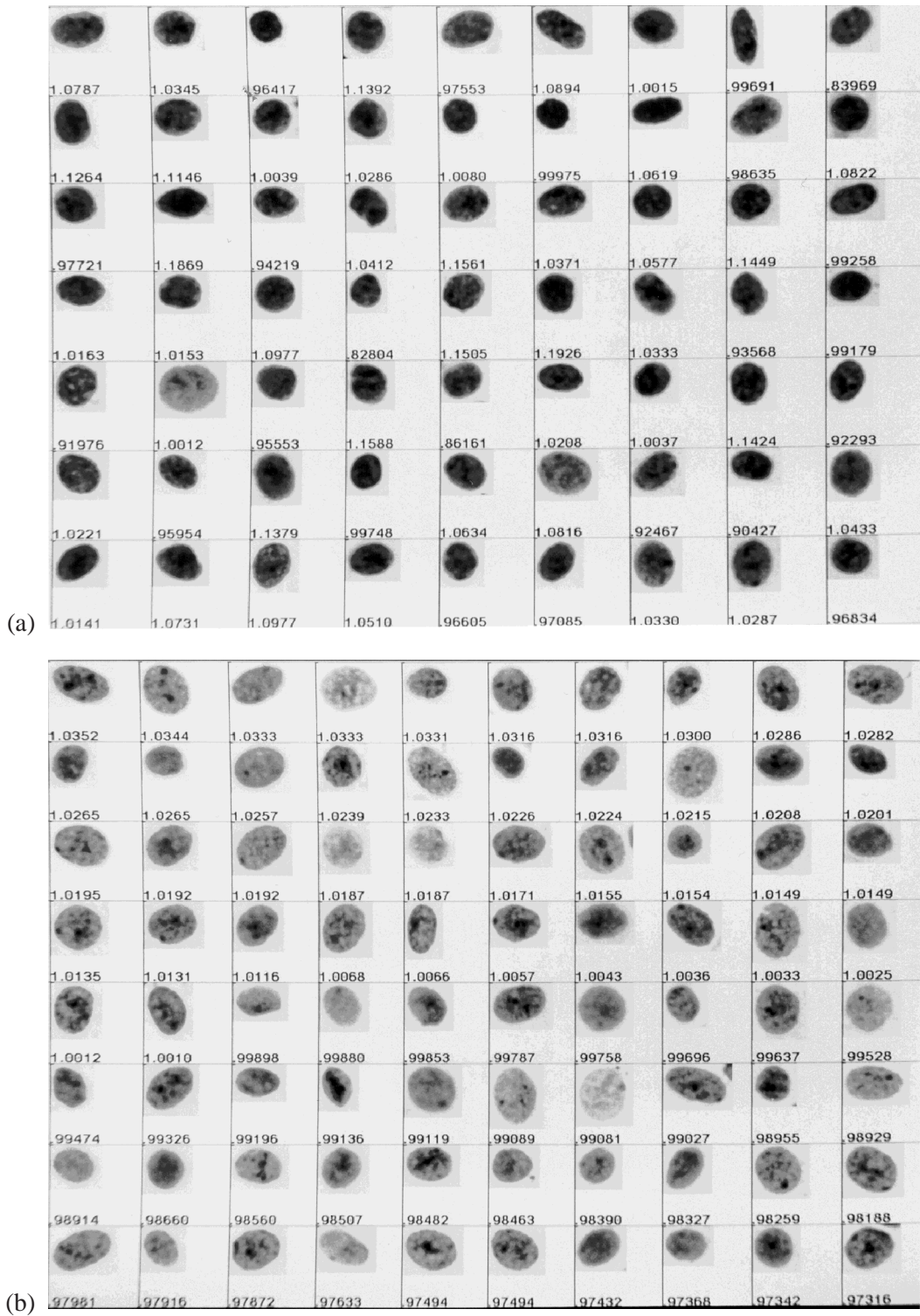
Fig. 4. Images of digitized nuclei of Feulgen-stained intermediate cells of (a) pro-CIN and (b) reg-CIN lesions.

3.3. DNA histograms

The plots of DNA index of all diagnostic cells from the (sub-)groups of progressive and regressive CIN lesions are shown in Fig. 5. The DNA index is the normalized value of the DNA content (IOD). There is little difference between reg-CIN and pro-CIN lesions. Reg-CIN lesions do show more heterogeneity. The results of DNA ploidy analysis in each of the smears from 26 progressive and 20 regressive CIN lesions with 15 or more diagnostic cells per specimen, are shown in Table 5. In the pro-CIN lesions DNA-diploidy did not occur. Eight (31%) pro-CIN lesions were classified as DNA-polyploid and 18 (69%) as DNA-aneuploid. DNA-diploidy was found in three (15%) reg-CIN lesions. Four (20%) reg-CIN lesions were classified as DNA-polyploid and 13 (65%) as DNA-aneuploid.

The mean and standard deviation of the histogram statistics over slides from the various diagnostic categories are presented in Table 5 for the following features of the DNA histograms: the 2.5c and 5c exceeding rates, mean DNA index, CV of DNA index, and entropy. None of the features shown exhibited a significant difference ($p > 0.1$) between pro-CIN and reg-CIN lesions, although their distributions were notably different. Cells exceeding 5c in DNA index are relatively rare in these lesions. The mean DNA index and 2.5c exceeding rate are higher in the progressive lesions, and tend to increase with CIN grade in both categories. The CV of the DNA index is higher within the regressive lesions, particularly in the regressive CIN III category.

4. Discussion

The most direct explanation for the significance of DNA-cytometric analysis in cervical dysplasia is afforded by observations that chromosomal aneuploidy, and the DNA-cytometric equivalent "DNA aneuploidy", may be regarded as a marker for neoplastic transformation [4]. It has been shown that the DNA profile of Feulgen-stained smears of the uterine cervix have significant prognostic information [2, 3,23,26]. A recent study of the DNA-cytometric feature N5C (the absolute number of cells with DNA content of more than 5c) of patients with cervical neoplasia showed that the N5C values significantly increased with increasing severity of CIN grade. However, the N5C values could not discriminate between the two groups: (1) CIN II or more, and (2) CIN I or less [30]. These findings are in

Table 5
DNA histogram statistics for cases with 15 or more diagnostic cells

| Feature	Statistic	Progressive lesions				Regressive lesions			
		CIN 1	CIN 2	CIN 3	Total	CIN 1	CIN 2	CIN 3	Total
2.5c exceeding	mean	0.80	0.82	0.83	0.82	0.69	0.65	0.77	0.71
	SD	0.27	0.20	0.19	0.22	–	0.36	0.30	0.32
5c exceeding	mean	0.04	0.02	0.06	0.04	0.00	0.06	0.11	0.08
	SD	0.04	0.04	0.12	0.07	–	0.07	0.21	0.03
Mean DNA index	mean	1.73	1.70	1.76	1.73	1.42	1.66	1.78	1.70
	SD	0.28	0.22	0.36	0.28	–	0.33	0.53	0.42
CV DNA index	mean	22	21	21	21	26	23	53	37
	SD	7.50	5.30	5.60	6.70	–	8.20	88	60
Entropy	mean	0.56	0.57	0.62	0.58	0.47	0.53	0.58	0.55
	SD	0.08	0.06	0.08	0.08	–	0.10	0.14	0.12
Diploidy	count	0	0	0	0	0	1	2	3
Polyploidy	count	4	2	2	8	0	4	0	4
Aneuploidy	count	7	5	6	18	1	5	7	13
Cases total		11	7	8	26	1	10	9	20
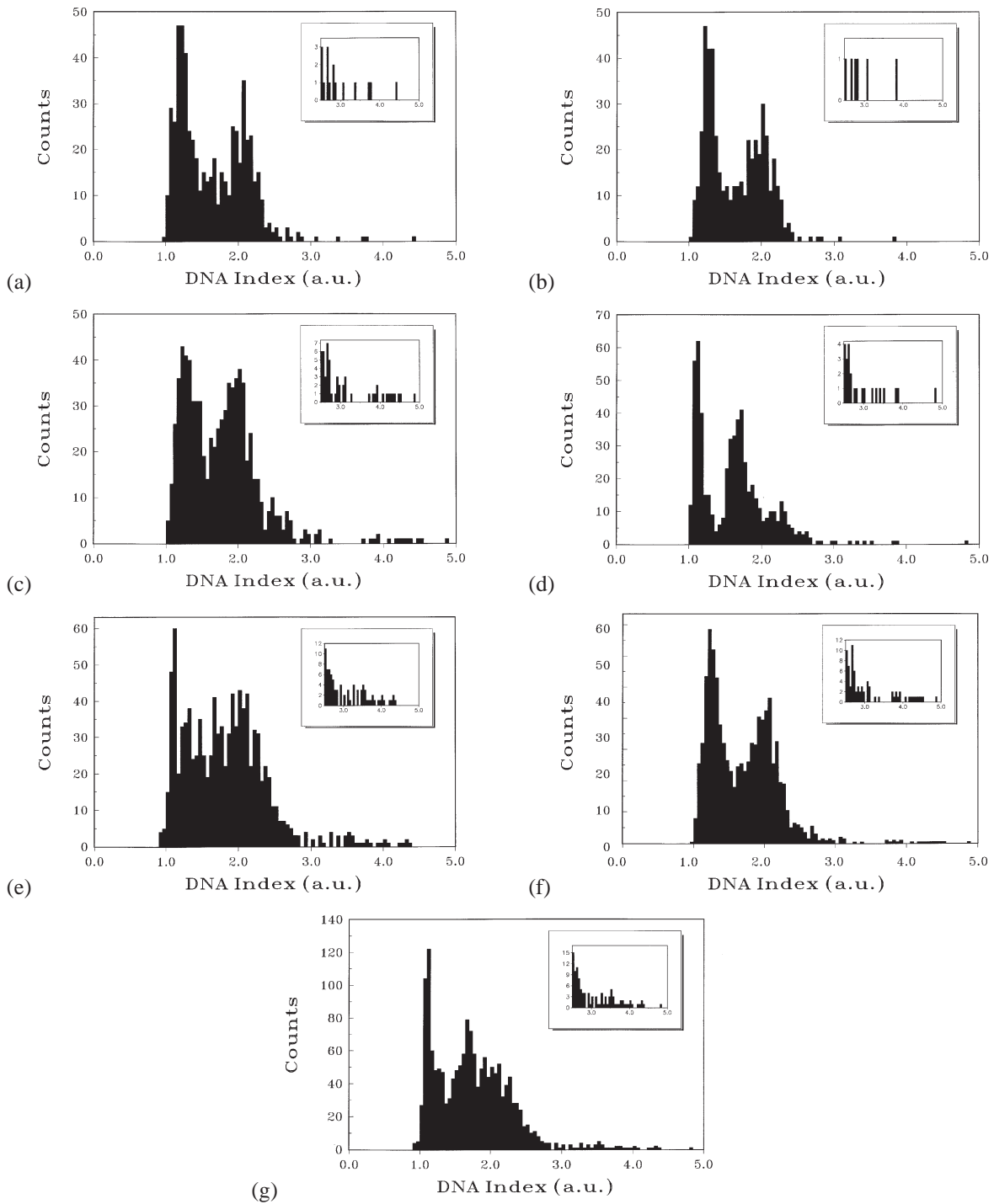
Fig. 5. Histograms of the DNA index of diagnostic cells from pro-CIN and reg-CIN lesions. The inset represents an expanded view of the region between DNA index 2.5 and 5. (a) CIN I progressive; (b) CIN II progressive; (c) CIN III progressive; (d) CIN I and II regressive; (e) CIN III regressive; (f) Progressive lesions combined from CIN I, II and III; (g) Regressive lesions combined from CIN I, II and III.

Table 6
Descriptive statistics for selected features of diagnostic cells

Feature	Progressive	Regressive
Mean values		
61 DNA index	1.70	1.76
10 mean radius*	15.50	14.90
63 OD max	0.426	0.517
66 low DNA amnt	0.244	0.225
67 med DNA amnt*	0.534	0.394
68 high DNA amnt	0.222	0.381
96 range extreme*	235	422
98 centre of gravity	0.039	0.038
103 fractal area 1	9850	7340
121 run length 90	205	202
Counts	1871	1592
Coefficients of variation		
61 DNA index	0.295	0.335
10 mean radius*	0.191	0.222
63 OD max	0.334	0.437
66 low DNA amnt	1.050	1.314
67 med DNA amnt*	0.460	0.647
66 high DNA amnt	1.245	0.929
96 range extreme*	0.395	0.432
98 centre of gravity	0.640	0.605
103 fractal area 1	0.367	0.445
121 run length 90	0.350	0.384

Features included in stepwise linear discriminant analysis are indicated with an asterick. Other features are listed for reference.

agreement with our previous results which showed that the 2.5c exceeding rate (ER) increased with increasing severity of the lesion [12]. In that study no relation could be found between the 2.5c ER and the progressive or regressive behavior of the CIN lesion. In the same study it was indicated that measurement of nuclear shape and chromatin texture features have the potential to provide a more sensitive indicator of progressive potential, as has been demonstrated in adenoma–carcinoma progression in colon [18].

With reference to the feature means in Table 6, it is possible to propose a translation of the diagnostic cell classifications into visually apparent light microscopical cytologic characteristics. It can be said that, on average, PAC$^+$ diagnostic cells are larger, with a significantly higher amount of DNA in regions of medium-condensed chromatin. There is an increase in the average run lengths detected in these cells, possibly due to the increases in the size of contiguous regions of medium condensed chromatin. The contrast of these cells is not as great as in PAC$^-$ cells, as reflected in both the OD max and range extreme parameters. The fractal area parameter indicates that the chromatin distribution is condensed in a more disorganized manner in PAC$^+$ cells, occupying significantly more surface area in the 3D plot of OD vs. x-y position.

For most variables the diagnostic cells from regressive lesions exhibit a marked increase in CV compared to measurements from the progressive cases, a heterogeneity which is also reflected in the histogram statistics in Table 5. In particular, the CIN III regressive lesions show a pronounced increase in CV of DNA index, as well as a quite large variation in this parameter from slide to slide. The 5c exceeding rate, mean DNA index, and entropy all show similar behavior for CIN III regressors. The reasons for this heterogeneity are not clear; these regressive lesions are evidently more advanced in their karyotypic evolution and yet have not developed the capacity to invade. A number of biological

Table 7
Descriptive statistics for feature measurements of intermediate cells

Variable	Progressive	Regressive
Mean values		
61 DNA index	0.988	0.991
16 mean radius	12.8	13.0
28 contrast	20.9	21.2
67 low DNA area	0.404	0.443
69 high DNA area	0.040	0.031
78 med av distance	0.594	0.587
86 high density objects	0.836	0.913
96 range extreme	221	241
Counts	7902	3828
Coefficients of variation		
61 DNA index	0.133	0.180
16 mean radius	0.101	0.101
28 contrast	0.274	0.258
67 low DNA area	0.485	0.459
69 high DNA area	1.720	1.171
78 med av distance	0.122	0.108
10 high density objects	1.160	1.120
96 range extreme	0.247	0.203

mechanisms may be invoked to explain this behavior, but it may also be true that CIN III regressors – representing the most extreme discordance between diagnosis and prognosis – do not constitute a consistent diagnostic category.

The analysis of intermediate cells proceeded in an analogous manner but yielded less resolution on a cell by cell basis in the differences between regressive and progressive lesions. Only a slight shift is evident between the main peaks in the plot of discriminant score in Fig. 3. For this reason it is more difficult to propose a translation of the discriminating cytometric variables to visually apparent cytologic features. The differences between progressive and regressive lesions are represented by shifts in the value of feature measurements over a large population of cells, and the overlap between the groups are quite large. It may be more reasonable to consider these differences as sub-visual, although with reference to Table 7 it might be said that intermediate cells from regressive lesions tend to be larger, with less extensive regions of high and medium-condensed chromatin. The range of the extreme parameter indicates that the contrast of the smaller highly condensed chromatin regions is greater in cells from regressive lesions. The Markovian parameters also indicate that the chromatin pattern is more irregular in cells from regressive lesions. All of these parameters are consistent with a more finely granular appearance of PAC$^-$ intermediate cells, which may be suggestive of some form of "reactive atypia". Although this cytologic category is not well understood, it is possible to speculate that this may be an important mechanistic aspect of CIN regression.

Slide classifications were obtained by applying a threshold to the number of PAC$^+$ cells present on the slide. For diagnostic cells, optimal accuracy (93%) is obtained if we concede that regressive lesions can have as many as 80% of diagnostic cells which are positive for PAC. Similarly, optimal accuracy (73%) is achieved for intermediate cells at the level where 40% of intermediate cells in regressive lesions exhibit PAC$^+$ features. These cutoff points are arbitrarily selected to afford the best classification accuracy, and should not be interpreted as the literal "burden" of PAC$^+$ cells. Rather these results indicate that there are large differences in feature distributions between reg-CIN and pro-CIN lesions, even though there is considerable overlap between these categories.

It is not straightforward to determine confidence limits for the use of thresholds to classify slides. It is a well-recognized problem in statistics that such procedures may tend to bias the results in favor of a more optimistic classification accuracy. It is important to emphasize that the statistical significance of this study is limited by the small number of cases, and that we do not propose at this point to have developed a classification scheme suitable for use in the setting of a screening program. A much larger, independent sample would be necessary in order to confirm these results. At a minimum this study does demonstrate that features of chromatin organization exhibit significant differences between progressive and regressive lesions. These differences are most convincingly evident in the diagnostic cells. If confirmed on a larger series of specimens these results may have significant implications for the management of CIN.

In the present study of 56 women with CIN we have shown that a discrimination between a progressive or regressive course of the disease is possible with 93% accuracy (slide classification). 96% of the diagnostic cells from pro-CIN lesions were correctly classified, and 100% of slides from pro-CIN slides were correctly classified using a threshold of 80% PAC$^+$ cells. The present findings are based on DNA measurements of just one Feulgen-stained specimen. It is possible that classifiers based on changes in cytometric features in two or more subsequent smears can further improve the sensitivity and specificity of the test. This hypothesis has been dictated by acquired knowledge regarding the existence of sequential cellular changes during the evolution of neoplasia, discriminating several phases of malignant transformation: (1) initiation, genetic instability, (2) focal aberrant proliferation, (3) focal dysplastic proliferation, (4) microinvasive growth, and (5) metastasis [6].

Based primarily on the analysis of colorectal and breast carcinoma, it has been proposed that in the majority (70%) of epithelial tumors, genetic instability is driven by what has been termed a "monosomic" pathway of chromosomal evolution [9,19,20]. This is characterized by a high frequency of chromosomal rearrangements, deletions of chromosome arms (less frequent duplication), and mitotic missegregation. The predominant karyotype is initially hypodiploid, but these cells possess a strong tendency towards endoreplication to hypotetraploidy, and subsequent development of "pseudotriploid" subclones with variable loss of duplicated chromosomes. Another subset of tumors (20–25%) has been characterized as "trisomic". Chromosomal rearrangements and deletions are more infrequent, and the most common abnormality is the duplication of entire chromosomes. There is relatively little tendency towards endoreplication and the development of polyploid side lines. A third category, comprising 5–7% of epithelial tumors, is characterized by only normal karyotypes, and has been linked to defects in replication error repair.

In cervical carcinoma karyotypic evaluations are scarce, but interphase cytogenetics using centromere enumeration probes has revealed aneusomies for a variety of chromosomes. In a recent study we have shown polyploidization of all investigated chromosomes occurs in progressive/persistent CIN lesions [7]. Furthermore, we have shown that progression from low grade towards high grade CIN lesions was accompanied by progressive increases in chromosome index (CI) for chromosomes 1, 7 and X, while for chromosomes 3, 6, 8, 11 and 17 no such correlation was found. Further progression towards invasive carcinoma of the cervix seems to be accompanied by specific chromosomal rearrangements.

According to a recently published CGH article [15], gain and amplification of sequences at 3q is associated with progression to invasive carcinoma in 90% of cases examined. Although it seems clear that this progressive genomic instability is correlated with classic changes in chromatin appearance in intra-epithelial neoplasia, there is little direct evidence for an impact of chromosomal rearrangements on the organization of chromatin in the interphase nucleus. A number of plausible mechanisms have been proposed but this remains a matter of speculation.

The most intriguing aspect of this study is that common differences in the chromatin patterns of progressive lesions are measurable in samples pooled from all diagnostic categories of CIN. This would seem to indicate that chromatin patterns exhibit an underlying indicator of progressive potential which is independent of the extent or severity of nuclear atypia. The potential for progression may not then be driven by the same processes which may underlie a putative progression of CIN through increasingly severe stages of CIN I, II and III.

It is also possible that this study merely underscores the shortcomings of the visual assessment of cytopathologic features of CIN. The discordance between diagnosis and prognosis, most extreme in the case of regressive CIN III lesions, may be due to the fact that the appropriate cues may be difficult if not impossible to evaluate in a subjective manner. In this respect it is likely that standardized measurement of chromatin configuration parameters will ultimately provide a more consistent basis for the assignment of risk to these lesions.

Acknowledgements

References

[1] G.H. Anderson, J.L. Benedet, J.C. LeRiche, J.P. Matisic and J.E. Thompson, Invasive cancer of the uterine cervix in British Columbia: A review of the demography and screening histories of 437 cases seen from 1985–1988, *Obstet. Gynecol.* **80** (1992), 1–4.

[2] M. Bibbo, H.E. Dytch, E. Alenghat, P.H. Bartels and G.L. Wied, DNA ploidy profiles as prognostic indicators in CIN lesions, *Am. J. Clin. Pathol.* **92**(3) (1989), 261–265.

[3] A. Böcking, DNA-cytometric diagnosis of prospective malignancy in borderline lesions of the uterine cervix, *Recent Results Cancer Res.* **122** (1991), 106–115.

[4] A. Böcking, DNA measurements: When and why?, in: *Compendium on Quality Assurance, Proficiency Testing and Workload Limitations in Clinical Cytology*, G.L. Wied, C.M. Keebler, D.L. Rosenthal, U. Schenck, T.M. Somrak and G.P. Vooijs, eds, Tutorials of Cytology, Chicago, IL, 1995.

[5] A. Böcking, F. Giroud and A. Reith, Consensus report of the ESACP task force on standardization of diagnostic DNA image cytometry, European Society for Analytical Cellular Pathology, *Anal. Cell. Pathol.* **8**(1) (1995), 67–74.

[6] C.W. Boone and G.J. Kelloff, Development of surrogate endpoint biomarkers for clinical trials of cancer chemoprevention agents: relationships to fundamental properties of preinvasive (intraepithelial) neoplasia, *J. Cell Biochem.* **19**(Suppl.) (1994), 10–22.

[7] J. Bulten, P.J. Poddighe, H. Robben, J.A. Gemmink, P.C.M. Wild and A.G.J.M. Hanselaar, Interphase cytogenetic analysis of cervical intraepithelial neoplasia, *Am. J. Pathol.* (1997, accepted for publication).

[8] A. Doudkine, C. MacAulay, N. Poulin and B. Palcic, Nuclear texture measurements in image cytometry, *Pathologica* **87** (1995), 286–299.

[9] B. Dutrillaux, Pathways of chromosome alteration in human epithelial cancers, *Adv. Cancer Res.* **67** (1995), 59–82.

[10] M. Guillaud, A. Doudkine, D. Garner, C. MacAulay and B. Palcic, Malignancy associated changes in cervical smears: systematic changes in cytometric features with gradc of dysplasia, *Anal. Cell. Pathol.* **9** (1995), 191–204.

[11] A.G.J.M. Hanselaar, G.P. Vooijs, B.H. Mayall, M.M.M. Pahlplatz and A.E. van't Hof-Grootenboer, DNA changes in progressive cervical intraepithelial neoplasia, *Anal. Cell. Pathol.* **4** (1992), 315–324.

[12] A.G.J.M. Hanselaar, G.P. Vooijs, A.E. van't Hof-Grootenboer, J.H. Gemmink, H. de Leeuw and M.M.M. Pahlplatz, Cytophotometric analysis of corresponding cytological and histological cervical intraepithelial neoplasia grade III specimen, *Cytometry* **12** (1991), 1–9.

[13] A.G.J.M. Hanselaar and G.P. Vooijs, Quality assurance in cytopathology in the Netherlands, in: *Compendium on Quality Control in Cytology*, G.L. Wied, ed., International Academy of Cytology, Chicago IL, 1994.

[14] A.L. Herbst, The Bethesda system for cervical/vaginal cytologic diagnoses, *Clin. Obstet. Gynecol.* **35**(1) (1992), 22–27.

[15] K. Heselmeyer, E. Schrock, S. du Manoir, H. Blegen, K. Shah, R. Steinbeck, G. Auer and T. Ried, Gain of chromosome 3q defines the transition from severe dysplasia to invasive carcinoma of the uterine cervix, *PNAS* **93**(1) (1996), 479–484.

[16] L.G. Koss, The Papanicolaou test for cervical cancer detection. A triumph and a treagedy, *JAMA* **261** (1989), 737–743.

[17] C. MacAulay and B. Palcic, An edge relocation segmentation algorithm, *Anal. Quant. Cytol. Histol.* **12**(3) (1990), 165–171.

[18] J.W. Mulder, G.J. Offerhaus, E.P. de Feyter, J.J. Floyd, S.E. Kern, B. Vogelstein and S.R. Hamilton, The relationship of quantitative nuclear morphology to molecular genetic alterations in the adenoma–carcinoma sequence of the large bowel, *Am. J. Pathol.* **141**(4) (1992), 797–804.

[19] M. Muleris, A. Almeida, M. Gerbault-Seureau, B. Malfoy and B. Dutrillaux, Identification of amplified DNA sequences in breast cancer and their organization within homogeneously staining regions, *Genes Chrom. Cancer* **14**(3) (1995), 155–163.

[20] M. Muleris, B. Zafrani, P. Validire, J. Girodet, R.J. Salmon and B. Dutrillaux, Cytogenetic study of 30 colorectal adenomas, *Cancer Genet. Cytogenet.* **74**(2) (1994), 104–108.

[21] H. Naujoks, R. Strohmeier, T. Bicker, A.M. van Driel-Kulker, C.F. Kpepfle and J.S. Ploem, Interobserver variability in the cytological diagnosis of 1500 Papanicolaou stained cervical monolayer specimens, *Pathol. Res. Pract.* **186**(1) (1990), 150–153.

[22] B. Palcic, C. MacAulay, S. Schlien, W. Treurniet, H. Tezcan and G. Anderson, Comparison of there different methods for automated classification of cervical cells, *Anal. Cell. Pathol.* **4**(6) (1992), 429–441.

[23] B. Palcic, D. Garner and C. MacAulay, Image cytometry and chemoprevention in cervical cancer, *J. Cell Biochem.* **23**(Suppl.) (1995), 43–54.

[24] J. Ponten, H.O. Adami, R. Bergstrom, L.G. Friberg, L. Gustaffson, A.B. Miller, D.M. Parkin, P. Sparen and D. Trichopoulos, Strategies for global control of cervical cancer, *Int. J. Cancer* **60** (1995), 1–26.

[25] A.E. Raffle, B. Alden and E.F. Mackenzie, Detection rates for abnormal cervical smears: what are we screening for?, *Lancet* **34**(8963) (1995), 1469–1473.

[26] R. Strohmeier, H. Naujoks, A.M. van Driel-Kulker and J.S. Ploem, Laboratory test of an automated cell analysis system for cervical screening, *Cytopathology* **4**(3) (1993), 139–147.

[27] M. van Ballegooijen, M.A. Koopmanschap and J.D. Habbema, The management of cervical intra-epithelial neoplasia (CIN): extensiveness and costs in the Netherlands, *Eur. J. Cancer* **31A**(10) (1995), 1672–1676.

[28] Y. van der Graaf, Screening for cervical cancer: The Nijmegen project, Thesis, University of Nijmegen, 1987.

[29] Y. van der Graaf, G.P. Vooijs and G.A. Zielhuis, Population screening for cervical cancer in the region of Nijmegen, The Netherlands, 1976–1985, *Gynecol. Oncol.* **30** (1988), 388–397.

[30] A.M. Van Leuwen, J.J. Ploem-Zaaijer, W.J. Pieters, H. Hollema and M.P. Burger, The suitability of DNA cytometry for the prediction of the histological diagnosis in women with abnormal cervical smears, *Br. J. Obstet. Gynecol.* **103**(4) (1996), 359–365.

[31] G.P. Vooijs, De adviserung bij afwijkende bevinginden van cytologisch onderzoek van de cervix uteri, *Ned. Tijdschr. Genccskd.* **131** (1987), 1662–1663.

[32] Ziekensfondsraad, Uitgangspunten herstructurering bevolkings onderzoek naar baarmoederhalskanker, Bestuit 592, Amstelveer, The Netherlands, 1993.